

# Wave–Packet Scattering off a Soliton

A.M.H.H. Abdelhady and H. Weigel

Physics Department, Stellenbosch University, Matieland 7602, South Africa

E-mail: abdelhady@sun.ac.za, weigel@sun.ac.za

**Abstract.** We investigate the scattering of a wave–packet off a soliton in the (1+1) dimensional kink model. We solve the classical, time-dependent field equation numerically subject to the initial condition that the wave–packet is widely separated from the kink solution at very early times and propagates towards the soliton. After some time the wave-packet interacts with the static soliton and departs from it at later times. At very late times the wave-packet is finally again separated from the soliton. We then extract the scattering matrix from the distorted wave-packet and compare it to the known result from the static scattering calculation. This constitutes a first step towards studying crossing symmetry in soliton models, i.e. in a framework beyond perturbation theory.

## 1. Introduction

Non–linear field theories often contain non–perturbative solutions with a localized energy density. These solutions are called *solitons* and are quasi–static in the sense that the center and the shape of the energy density have simple time dependences. These soliton solutions [1] possess a wide range of applications in physics. To present an incomplete list, this range covers cosmology [2, 3], particle and nuclear physics [4, 5], as well as condensed matter physics [6]. The prototype soliton model is the kink in one time and one space dimension for the real scalar field  $\phi$

$$\mathcal{L} = \frac{1}{2} \partial_\mu \phi \partial^\mu \phi - \frac{\lambda}{4} \left( \phi^2 - \frac{M^2}{2\lambda} \right)^2. \quad (1)$$

Here  $M$  is the mass parameter and  $\lambda$  is the coupling constant. The equation of motion reads

$$\ddot{\phi}(x, t) = \phi''(x, t) - \lambda \left( \phi^2(x, t) - \frac{M^2}{2\lambda} \right) \phi(x, t). \quad (2)$$

For simplification we have introduced the partial derivatives  $\dot{\phi} = \partial\phi/\partial t$  and  $\phi' = \partial\phi/\partial x$ . The kink soliton

$$\phi_K(x) = \frac{M}{\sqrt{2\lambda}} \tanh \left( \frac{M}{2} x \right). \quad (3)$$

is a static solution to eq. (2) with boundary conditions at spatial infinity that connect the two vacuum configurations  $\phi_0 \equiv \pm \frac{M}{\sqrt{2\lambda}}$ . They arise from the spontaneous breaking of the reflection symmetry  $\phi \leftrightarrow -\phi$ . Time dependent solutions can easily be constructed by an appropriate Lorentz transformation [1]. Typically small amplitude fluctuations  $\eta(x, t)$  about the solution,

$\phi(x, t) = \phi_K(x) + \eta(x, t)$  are introduced to quantize this classical configuration. The first non-trivial order of the expansion in powers of the wave-function  $\eta(x, t)$  yields a Schrödinger type equation with a potential induced by the kink. Standard techniques [1] yield the momentum dependent phase shift

$$\delta(k) = 2\arctan\left(\frac{3Mk}{2k^2 - M^2}\right). \quad (4)$$

for the scattering solution. In addition there are two bound state solutions with energies  $\sqrt{3}M/2$  and  $\sqrt{2}M$ . Here we present a calculation for this phase shift that is based on the direct solution of the equation of motion (2) in coordinate space with suitable initial conditions that reflect the physical situation of particle scattering. These methods can then be utilized to study features beyond the small amplitude approximation. Most of the results presented here are part of a more comprehensive paper [7].

## 2. Wave-Packet

We want to simulate the scattering of a particle off the kink. To this end we consider a localized wave-packet that represents the particle far away from the kink. We impose initial conditions such that the wave-packet propagates towards the kink, interacts with it and then moves away from it. Finally we extract the scattering data (in particular the phase shift) from the structure of the wave-packet at a very late time.

We build the wave-packet as a superposition of solutions to the free equation of motion in the small amplitude approximation. These solutions are plane waves with the dispersion relation  $\omega_k = \sqrt{k^2 + M^2}$ ,

$$\eta_{\text{wp}}(x) = \int_{-\infty}^{\infty} dk A(k) e^{ikx}. \quad (5)$$

At  $t = 0$  the dispersion relation enters only via the velocity of the initial wave-packet

$$\dot{\eta}_{\text{wp}}(x) = -i \int_{-\infty}^{\infty} dk \omega_k A(k) e^{ikx}. \quad (6)$$

In the context of our numerical simulations we assume the spectral function in momentum space to be of Gaussian shape

$$A(k) = a_0 e^{-\frac{(k-k_0)^2}{\sigma_k^2}}, \quad (7)$$

where  $a_0$  is the amplitude,  $k_0$  is the average momentum, and  $\sigma_k$  is the width of the distribution. This wave-packet defines the initial configuration

$$\phi(x, 0) = \phi_{\text{bg}}(x - x_0) + \eta_{\text{wp}}(x) \quad \text{and} \quad \dot{\phi}(x, 0) = \dot{\eta}_{\text{wp}}(x) \quad (8)$$

for integrating the time-dependent equation of motion (2). The background configuration can be either the trivial vacuum,  $\phi_{\text{bg}}(x) = \frac{M}{\sqrt{2}\lambda}$  or the kink,  $\phi_{\text{bg}}(x) = \phi_K(x)$  and  $x_0 > 0$  denotes the position of its center. The small amplitude approximation can be neatly parameterized by the limit  $a_0 \rightarrow 0$ . For sufficiently large  $k_0$  the wave-packet will travel towards the background and will interact with it within a finite time interval [8].

For small enough  $a_0$  the solutions in the kink background at late times (after the interaction with the kink is completed so that the overlap between the kink and the wave-packet can be safely ignored) are

$$\phi(x, t) = \phi_K(x - x_0) + \int_{-\infty}^{\infty} dk A(k) \exp[i(kx - \omega_k t + \delta(k))] + \mathcal{O}(a_0^2). \quad (9)$$

We may converse this line of argument to extract the phase shift from the solution

$$\eta_{\text{wp}}^{(S)}(x, t) = \phi(x, t) - \phi_{\text{K}}(x - x_0) \quad (10)$$

to the equation of motion with initial conditions, eq. (8) at very late times  $t_f \gg 0$ ,

$$e^{i\delta(k)} = \frac{e^{i\omega_k t_f}}{A(k)} \int_{-\infty}^{\infty} \frac{dx}{2\pi} e^{-ikx} \eta_{\text{wp}}^{(S)}(x, t_f). \quad (11)$$

The dependence on  $t_f$  will cancel, at least in the small amplitude approximation.

Though the initial configuration is motivated by the small amplitude approximation, we emphasize that our solutions to the time-dependent equation of motion are not restricted to this condition.

### 3. Numerical Results

Before addressing details of the numerical results, we remark that conservation of the total energy

$$E = \int_{-\infty}^{\infty} dx \epsilon(x, t) \quad \text{with} \quad \epsilon(x, t) = \frac{1}{2} \left( \dot{\phi}^2(x, t) + \phi'^2(x, t) \right) + \frac{\lambda}{4} \left( \phi^2(x, t) - \frac{M^2}{2\lambda} \right)^2 \quad (12)$$

is the most important criterion for accepting a numerical solution. Note that the above mentioned initial conditions yield a complex field  $\phi(x, t)$  and so is the corresponding energy. In eq. (12) we have also made explicit the time-dependent energy density,  $\epsilon(x, t)$ .

All results presented in this section will be measured with respect to the dimensionless quantities on the right hand side of

$$(x, t) \longrightarrow \frac{(x, t)}{\sqrt{2} M} \quad \text{and} \quad \phi \longrightarrow \frac{M}{\sqrt{2} \lambda} \phi. \quad (13)$$

Then a plane wave has mass  $\sqrt{2}$ . In figure 1 we present the physical energy density for the time-dependent solution that is characterized by restricting the initial wave-packet to its real part. To single out the wave-packet we particularly consider  $\bar{\epsilon}(x, t) = \epsilon(x, t) - \frac{1}{2} \left[ 1 - \tanh^2(x - x_0) \right]^2$ , where the subtraction refers to the energy density of the kink. Though we can clearly identify the propagation of the wave-packet, we also recognize an unexpected residual structure at the center of the kink. It represents a displacement of the kink [7]. This displacement increases with the initial amplitude  $a_0$  and corresponds to an attraction shortly before and a repulsion shortly after the interaction with the wave-packet. The displacement can also be observed from the actual configuration in figure 2, where we display the real part of the solution to the equation of motion with complex initial conditions (8) with the kink background. The imaginary part exhibits a similar behavior, merely phase shifted by  $\pi/2$ . We can clearly identify the three phases of the propagation of the wave-packet: First the propagation of the wave-packet towards the kink, second the interaction as the wave-packet climbs up the kink, and third the distorted wave-packet moving away from the kink. From the field configuration in the third phase we will eventually extract the phase shift via eq. (11). Unfortunately there is a number of numerical obstacles that we need to overcome first.

To begin with, we have to incorporate the above mentioned displacement of the kink in the integral, eq. (11). This is straightforwardly accomplished by restricting the integration interval to the regime of the wave-packet. For very late times ( $t_f > 100$ ) this regime is clearly separated from the kink. Other obstacles are more cumbersome. Wave-packet components with small

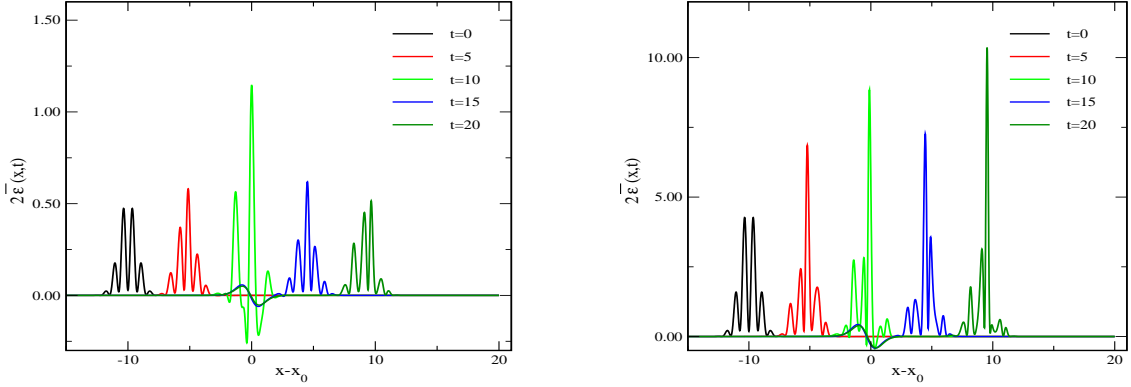


**Figure 1.** (Color online) Time snapshots of the energy density  $\bar{\epsilon}(x, t)$  (in  $M^4/8\lambda^2$ ) of the wave-packet for real initial conditions. We have used  $k_0 = 4$  and  $\sigma_k = 2$ . Left panel:  $a = 0.05$ , right panel:  $a = 0.15$ . Note the different scales on the ordinate.

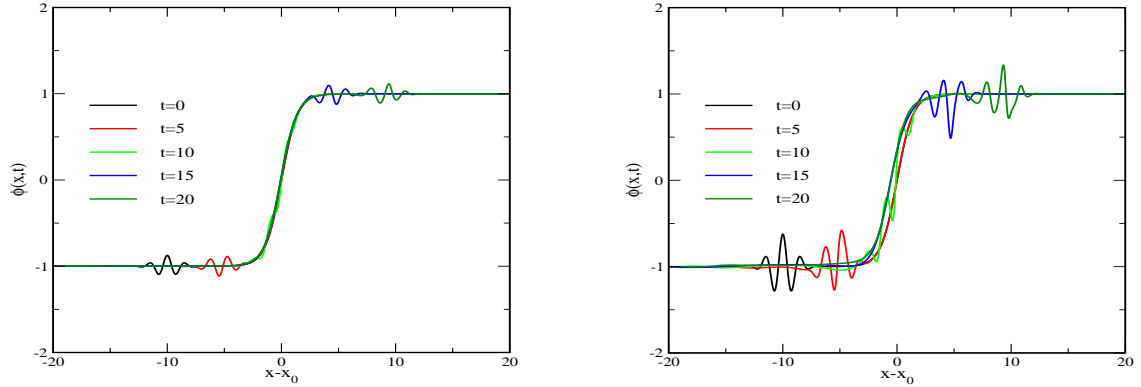


**Figure 2.** (Color online) Time snapshots of the real part of the field configuration in the kink background.

momenta take a long time to finalize the interaction with the kink. Hence we need to solve the equation of motion for a large interval on the time axis. We consider  $t \in [0, 200]$  but also vary the upper limit to ensure stability of the results. However, components with large momenta will propagate a long distance in the same time interval. Hence we also need to consider a large interval in coordinate space. In order to reliably find the Fourier transform in eq. (11) we require a dense grid in coordinate space for large momentum components. This increases the numerical cost additionally. To keep the numerical effort within a manageable range, it is therefore appropriate to split the computation in (at least) two regimes in momentum space. To extract the phase shift for small momenta, we consider a large time interval but a small interval in coordinate space. This leads to unreliable results at large momenta. For that regime we consider a small time interval but a large one in coordinate space; together with a dense grid. At intermediate momenta the two procedures yield identical results. Furthermore we have the freedom to tune the parameters of the wave-packet,  $k_0$  and  $\sigma_k$  to suit the considered regime in momentum space. These regimes of different numerical treatments are indicated in figure 3.

We also display the numerical result for the imaginary part of the right hand side of eq. (11). Its deviation from unity serves as a further test on the numerical accuracy. As expected this occurs for very small and very large momenta. Otherwise the agreement with the analytical

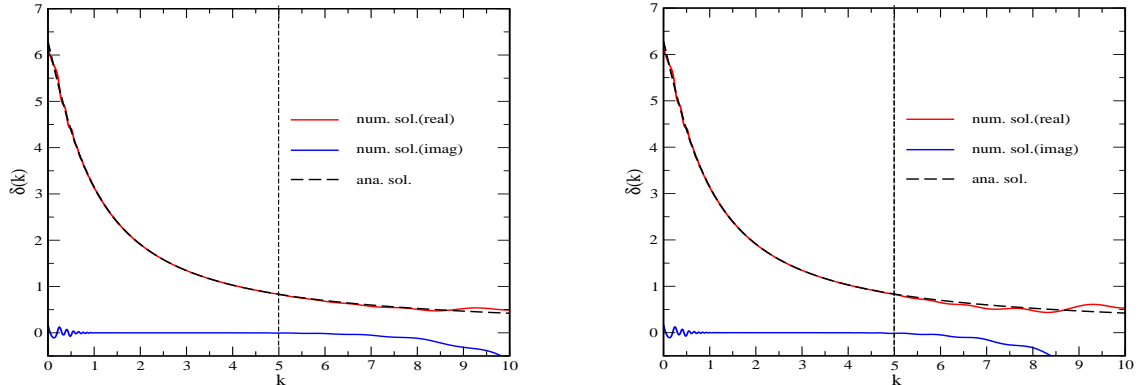


**Figure 3.** (Color online) Phase shifts extracted from the interaction between the kink and the wave-packet with amplitude  $a_0 = 0.05$  (left) and  $a_0 = 0.15$  (right). The vertical line indicate different numerical treatments as discuss in the text.

result, eq. (4) is astonishing. Certainly, further segmentation of the momentum axis and optimization in each segment will yield even better agreement. We have obtained the result displayed in figure 3 for  $a_0 = 0.05$  in which case the small amplitude approximation is expected to be accurate. Figure 3 shows that we find identical phase shifts also for larger amplitudes,  $a_0 \approx 0.15$ . Though our computations show deviations from the small amplitude approximation in the imaginary part of the phase shift, we believe them to be short-comings of the numerical procedure and conclude that the scattering data do not exhibit non-linear effects even at moderate amplitudes.

#### 4. A non-linear effect

Above we have already identified the displacement of the kink as a non-linear effect. This does not occur in the small amplitude approximation. However, as we increase the amplitude of the wave-packet the center of the kink gets slightly shifted towards the initial position of the wave-packet. As we further increase the amplitude, the sign of the displacement changes and eventually the kink co-moves with the (dominant piece of the) wave-packet after the interaction. This effect is clearly seen in figure 4 where we display both, the real parts of the subtracted energy density and the field as functions of time. In addition we observe that the wave-packet splits into various pieces that propagate with different velocities. This appears to be an indication of particle production.

#### 5. Conclusion

The phase shift for the scattering of small fluctuations about the kink soliton has been known for quite a while. We have reconstructed this phase shift via the time-dependent simulation of the collision between the kink and a wave-packet of small and moderate amplitude. By choosing a significantly wide initial spectral function this turned possible by a single integration of the equation of motion, although numerical accuracy can be improved by optimizing both, numerical parameters as well as initial conditions to a particular momentum regime.

The wave-packet approach is more descriptive of the scattering process than the small amplitude approach. In addition this technique captures non-linear effects. Since the initial wave-packet is localized this numerical simulation also preserves the topological charge of the kink.

We have established that the wave-packet drags the kink after the collision for sufficiently

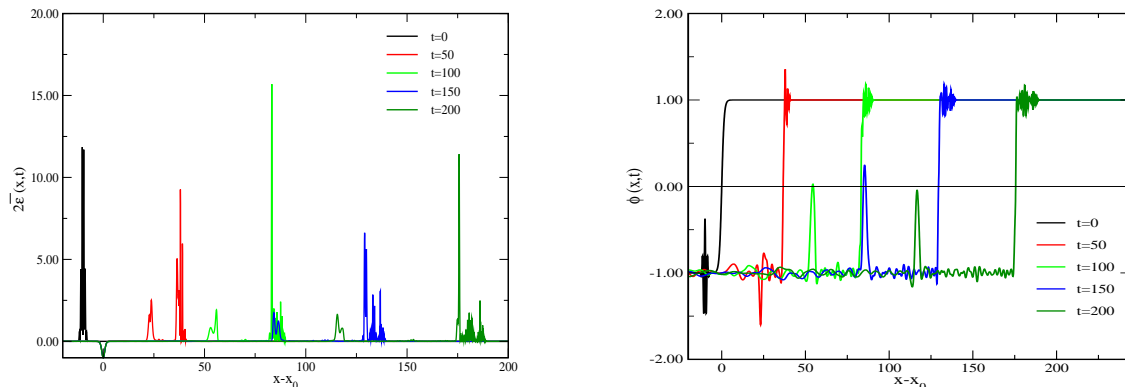


**Figure 4.** (Color online) Results for real initial conditions using  $a_0 = 0.25$ . Left panel: subtracted energy density  $\bar{\epsilon}(x, t)$ , right panel: field configuration  $\phi(x, t)$ .

large amplitudes. Furthermore the wave-packet splits into several pieces in this non-linear regime. These occur to be so far unknown features of the model.

The successful reproduction of the phase shift for scattering off the kink from the time-dependent equation of motion in configuration space is the first step towards establishing crossing symmetry in topological soliton model. The next step consists of assuming an initial condition that describes colliding kink-antikink configurations [9, 10] and relating the time-dependent field configuration to the one discussed here.

### Acknowledgments

One of us (AMHHA) is supported in parts by the African Institute for Mathematical Sciences (AIMS).

### References

- [1] R. Rajaraman, *Solitons and Instantons*. North Holland, Amsterdam (1982).
- [2] A. Vilenkin and E.P.S. Shellard, *Cosmic Strings and other Topological Defects*, Cambridge University Press, Cambridge (UK), 1994.
- [3] T. Vachaspati, *Kinks and domain walls: An introduction to classical and quantum solitons*, Cambridge University Press, Cambridge (UK), (2006).
- [4] N. Manton and P. Sutcliffe, *Topological Solitons* Cambridge University Press, Cambridge, (UK), (2004).
- [5] H. Weigel, *Lect. Notes Phys.* **743** (2008) 1.
- [6] A. R. Bishop and T. Schneider (Eds.), *Solitons in Condensed Matter Physics*, Springer Verlag, Berlin (1978).
- [7] A. M. H. H. Abdelhady and H. Weigel, “Wave-Packet Scattering off the Kink-Solution”, arXiv:1106.3497.
- [8] W. Hasenfratz and R. Klein, *Physica* **89A** (1977) 191.
- [9] S. V. Demidov and D. G. Levkov, *JHEP* **1106** (2011) 016 [arXiv:1103.2133 [hep-th]].
- [10] T. Romanczukiewicz and Y. Shnir, *Phys. Rev. Lett.* **105** (2010) 081601 [arXiv:1002.4484 [hep-th]].